Received: 30 October 2023 | Revised: 20 December 2023 | Accepted: 22 December 2023

DOI: 10.1002/pol.20230810

RESEARCH ARTICLE

JOURNAL OF POLYMER SCIENCE WILEY

Effect of self-seed crystal structure on growth of polymorphs in poly(butylene 2,6-naphthalate): A cross-nucleation study

Mengxue Du[1] | **René Androsch**[1] | **Dario Cavallo**[2]

[1]Interdisciplinary Center for Transfer-oriented Research in Natural Sciences, Martin Luther University Halle-Wittenberg, Halle/Saale, Germany

[2]Department of Chemistry and Industrial Chemistry, University of Genova, Genova, Italy

Correspondence
René Androsch, Interdisciplinary Center for Transfer-oriented Research in Natural Sciences, Martin Luther University Halle-Wittenberg, 06099 Halle/Saale, Germany.
Email: rene.androsch@iw.uni-halle.de

Dario Cavallo, Department of Chemistry and Industrial Chemistry, University of Genova, Via Dodecaneso 31, 16146 Genova, Italy.
Email: dario.cavallo@unige.it

Funding information
Deutsche Forschungsgemeinschaft, Grant/Award Number: AN 212/29; Martin Luther University Halle-Wittenberg

Abstract

Cross-nucleation between different crystal polymorphs is a particular, self-seed assisted type of heterogeneous nucleation, where a fast-growing polymorph nucleates at a pre-existing crystal surface of another polymorph. Here, we present a study on cross-nucleation between different crystalline phases of poly(butylene 2,6-naphthalate) (PBN), employing hotstage polarized-light optical microscopy and temperature-resolved wide-angle X-ray scattering as analysis tools. PBN forms α-crystals at relatively low temperature and β′-crystals at rather high temperature, with cross-nucleation experiments designed such to first obtain few α- or β′-seed crystals (mother phase) which then are transferred to higher or lower temperature, respectively, to monitor the continuation of the crystallization process and possible growth of the other polymorph. In case of cooling β′-crystals to lower temperature where typically α-crystals form in the non-seeded isotropic melt, β′-crystals nucleate growth of α-crystals, following many examples of cross-nucleation in the literature. In contrast, if low-temperature-generated α-crystals are heated to a temperature where β′-crystals form in a non-seeded melt, the cross-nucleation efficacy is reduced as, beside growth of cross-nucleated β′-crystals, also growth of the mother phase is observed. This unexpected result demonstrates the importance of the structure of the nucleating substrate and the interplay between kinetic and thermodynamic aspects of crystal growth.

KEYWORDS

cross-nucleation, crystal nucleation, crystal polymorphism, crystallization, poly(butylene 2,6-naphthalate)

1 | INTRODUCTION

Controlling crystal polymorphism in crystallizable polymers, that is, controlling the ability to obtain specific crystal structures is a great challenge in material science since the different arrangements of the molecules in the crystalline solid state ultimately control the final material properties. Examples include the melting temperature,[1,2] the mechanical behavior,[3–5] or piezoelectric properties.[6,7] Most straightforward for obtaining a specific crystal

polymorph in a single-component system is the selection of proper crystallization conditions in terms of temperature and pressure, that is, following the information of equilibrium phase diagrams, which, however, often are not available. This notwithstanding, for many polymers knowledge about the effect of crystallization temperature and cooling rate (in case of hot-crystallization), or heating rate (in case of cold-crystallization) on the generation of specific crystal polymorphs—regardless whether being the thermodynamically most stable phase, or not—is available.

Polymer crystallization follows the general scheme of crystal nucleation, growth, and perfection.[8] Crystallization of the bulk melt requires homogeneous nucleation,[9] with details of the structure, including the arrangement of molecular segments within the nuclei and the surface structure, still unknown. However, it appears that the surface structure of homogenous nuclei does not control the selection of a specific crystal polymorph, as after their transfer to different growth temperatures, according to Tammann's two stage crystal nuclei development method,[10,11] different crystal structures may form.[12] Similarly, in case of heterogeneous nucleation, that is, nucleation of the growth process by pre-existing surfaces, observations indicate that the (foreign) surface structure may be of low importance regarding the structure of the growing crystal, as crystallographic matches typically are not evident. However, on the other side, careful selection of purposely-added nucleating agents with a specific crystal structure allows epitaxial growth of polymorphs, with the β-phase of isotactic polypropylene (iPP) being a prominent example.[13,14]

A special type of heterogeneous nucleation is the growth of crystals on surfaces of the same species, often denoted as self-seeding.[15–17] In the context of controlling crystal polymorphism, so-called cross-nucleation experiments were designed, for analyzing whether seed-crystals (mother phase) are able to nucleate growth of a different polymorph (daughter phase). Such studies were performed on both small molecules,[18,19] for which this nucleation mechanism was identified being relevant, for example, for producing specialty chemicals, and on polymers, including investigations on poly(1,3-dioxolan),[20] branched polyethylene,[21] poly(butene-1) (iPB-1),[22,23] or poly(pivalolactone)[24] to name only a few; more examples are provided in a recent review.[25] These dedicated cross-nucleation studies on polymers, however, were advanced by earlier observation of this phenomenon when detecting a so-called growth transformation in isotactic polypropylene (iPP), with nucleation/growth of trigonal β-crystals at the growth front of α-crystals in a temperature gradient.[26]

Research of cross-nucleation of polymers between polymorphs suggests that this process is not primarily controlled by the relative thermodynamic stability of the different polymorphs. Rather than it appears that at the cross-nucleation temperature the growth rate of the daughter phase needs to be higher than that of the nucleating mother phase. However, this growth-rate prerequisite may not cause cross-nucleation in any case, as further, yet unknown conditions need to be fulfilled.[19,25] Furthermore, it seems that matching of the crystal lattices of the cross-nucleating polymorphs is of low importance, although for iPB-1 epitaxy between the cross-nucleating structures has been demonstrated.[27] For example, while in iPP the chain-conformation of mother (β-crystals) and daughter phases (α-crystals) are identical, in case of Form II-on-Form I cross-nucleation in iPB-1 those are different.[22,25,28]

Therefore, some intriguing questions on this peculiar heterogeneous nucleation process between polymorphs remain, and the exploration of other polymorphic systems will be beneficial for its further understanding. To this aim, in this manuscript we present results on the cross-nucleation between the different crystalline phases of poly(butylene 2,6-naphthalate) (PBN).

PBN displays a rich polymorphic behavior, including two crystalline and one smectic liquid crystalline phases.[29] Regarding the latter, the smectic mesophase develops upon cooling the melt at high rates,[30] and it is an intermediate state for the formation of the crystalline α-modification, according to the Ostwald's rule of stages.[31–34] However, of interest in the present investigation are the two crystalline β′- and α-polymorphs, which both exhibit a simple triclinic unit cell accommodating one chain repeat unit. The fiber repeat distance of the β′-structure is slightly larger than that of the α-polymorph, which is caused by different conformations of the butylene sequence of the chain repeat unit and different degree of co-planarity of the ester groups and the naphthyl rings.[35,36] The crystal density of the β′-phase is slightly higher than that of the α-phase, and its equilibrium melting temperature is reported 281°C, about 20 K higher than that of the α-phase.[37] The β′-crystal polymorph forms exclusively at low supercooling of the melt, at temperatures higher than about 220–230°C, or on cooling at rates well below 1 K/min. With increasing cooling rate and supercooling of the melt, formation of the β′-phase is progressively replaced by growth of α-crystals, and below about 200°C development of β′-crystals is completely absent.[38,39] As such, simultaneous crystallization of the two polymorphs is obtained for crystallization temperatures between, roughly, 200 and 230°C, however, without any further information about the mechanism behind. The two crystal polymorphs present different supermolecular structures, which are well distinguishable by polarized-light optical microscopy (POM). The slow growth of isolated and rather long/needle-like β′-crystals leads to the formation of a dendritic

spherulite morphology superstructure, while the α-phase develops typical negative spherulites, at least on hot-crystallization.[39–41] As expected, cold-crystallization and crystallization from an oriented melt leads to different morphologies,[42,43] which, however, are out of interest in the present work.

Cross-nucleation in PBN is not yet explored, though early experiments proved the possibility of generation of co-existing semicrystalline morphologies, by incomplete high-temperature crystallization, to obtain β′-crystals first, and rapid cooling of the system to a temperature where α-spherulites grew.[41] In this experiment, a comparison of the μm-scale organization of the different crystal polymorphs was in foreground, and not possible nucleation of α-crystal growth at the boundary of β′-spherulites. To shed further light on open questions of cross-nucleation in polymorphic polymers, including whether a growth-rate difference is sufficient to change the crystal structure during continued growth of the seed (mother) crystals after a change of the crystallization temperature, or whether there exist further constraints, in this study PBN is analyzed. First, information about the temperature-dependence of growth rates of the two polymorphs of interest are provided, which then is followed by presentation of cross-nucleation experiments, with both, β′- and α-crystals serving as mother phase. As analytic tools we used hotstage POM and temperature-resolved wide-angle X-ray scattering (WAXS), with the latter applied to assure the formation of specific crystal polymorphs.

2 | EXPERIMENTAL

2.1 | Material

Additive-free PBN pellets with an intrinsic viscosity of 0.92 dL/g, measured at 30°C using a 60:40 m/m% mixture of phenol and 1,1,2,2-tetrachloroethane, were obtained from Teijin Shoji Europe GmbH (Hamburg, Germany) and used as received.[33]

2.2 | Instrumentation

2.2.1 | Polarized-light optical microscopy (POM)

Morphological analyses were made on approximately 10 μm thin polymer slices, obtained from the pellets using a rotary microtome (Slee medical GmbH, Nieder-Olm, Germany). For microscopic observations, we used a DMRX microscope (Leica, Wetzlar, Germany) equipped with a CCD camera and connected to a THMS600 hotstage (Linkam, Tadworth, UK). Samples were placed between crossed polarizers and monitored in transmission mode.

2.2.2 | Wide-angle X-ray scattering (WAXS)

Measurements were performed in transmission mode employing a Retro-F laboratory setup (SAXSLAB, Copenhagen, Denmark) using a microfocus X-ray source and an ASTIX multilayer X-ray optics (AXO Dresden GmbH, Dresden, Germany) as monochromator, providing CuKα radiation (wavelength 0.154 nm). The size of the double-slit generated X-ray beam was about 0.9 mm, and the intensity of the scattered X-rays was measured by a 2D PILATUS3 R 300K detector (DECTRIS Ltd., Baden, Switzerland), with the 2D-X-ray patterns azimuthally averaged to obtain the intensity as a function of the scattering angle 2θ. Preparation of samples for X-ray analysis included in a first step compression-molding of films of about 200 μm thickness with a film-maker accessory (Specac Ltd., Orpington, UK) in combination with a heatable hydraulic press (LOT QD, Darmstadt, Germany). After adjustment of the lateral dimension, a specimen was inserted into a 20 μL-aluminum pan (Mettler-Toledo, Greifensee, Switzerland), which, finally, was attached onto the silver-block of an HFS350 hotstage (Linkam, Tadworth, UK), serving as sample holder in the X-ray setup. Importantly, for accurate monitoring of the sample temperature, a chromel-alumel μ-thermocouple (Omega Engineering GmbH, Deckenpfronn, Germany) was attached on the aluminum lid of the sample pan, using a fast OM-DAQXL-1-EU data logger (Omega Engineering GmbH, Deckenpfronn, Germany) for readout.

3 | RESULTS AND DISCUSSION

3.1 | Spherulite growth rate

Pre-requisite for definition of thermal protocols for cross-nucleation experiments is knowledge about temperature ranges in which α- and β′-crystals grow. Though general information is already available in the literature,[38,39] such that α- and β′-crystal growth is expected at temperatures, roughly, below and above about 220–230°C, respectively, for the specific PBN grade of this work, data are absent. In addition, to the best of our knowledge, information about the temperature-dependence of the growth rate of α- and β′-crystals in lateral direction are also not reported yet, though crystal growth rates are needed for interpretation of possible cross-nucleation; only a single spherulite growth-rate value for crystallization at 220°C has been

reported.[44] For these reasons, hotstage POM was applied to gain the necessary knowledge.

Figure 1 presents the evolution of the spherulite morphology of PBN isothermally crystallized at rather low temperatures of 210 (bottom row), 215 (center row), and 220°C (top row), with the images shown from the left to the right captured after different crystallization time, as indicated. At temperatures of 210 and 215°C, typical PBN α-phase spherulites are observed, as evidenced by the distinct Maltese cross pattern. The spherulites exhibit negative birefringence, which suggests a lamellar morphology of radially grown crystals, with the chain axis oriented perpendicular to the spherulite radius. Regarding the growth rate, it can be clearly seen that it increases with decreasing crystallization temperature, as spherulites of comparable sizes are obtained in much shorter times at 210°C, with respect to 215°C. Similarly, as expected, the nucleation density is also affected by the crystallization temperature, being slightly increased for crystallization at 210°C. At the highest crystallization temperature of 220°C, the spherulites seem to be darker than spherulites obtained at lower crystallization temperature, showing a spotty pattern in its interior. Based on the knowledge of the morphology of PBN containing β′-crystals,[39,40] the images suggest that at this temperature a mixed morphology, comprising both α- and β′-crystals developed.

Figure 2 reports the morphology development during isothermal crystallization at lower supercooling of the melt, at temperatures from 225 (bottom row) to 240°C (top row). A clear change of the spherulite morphology,

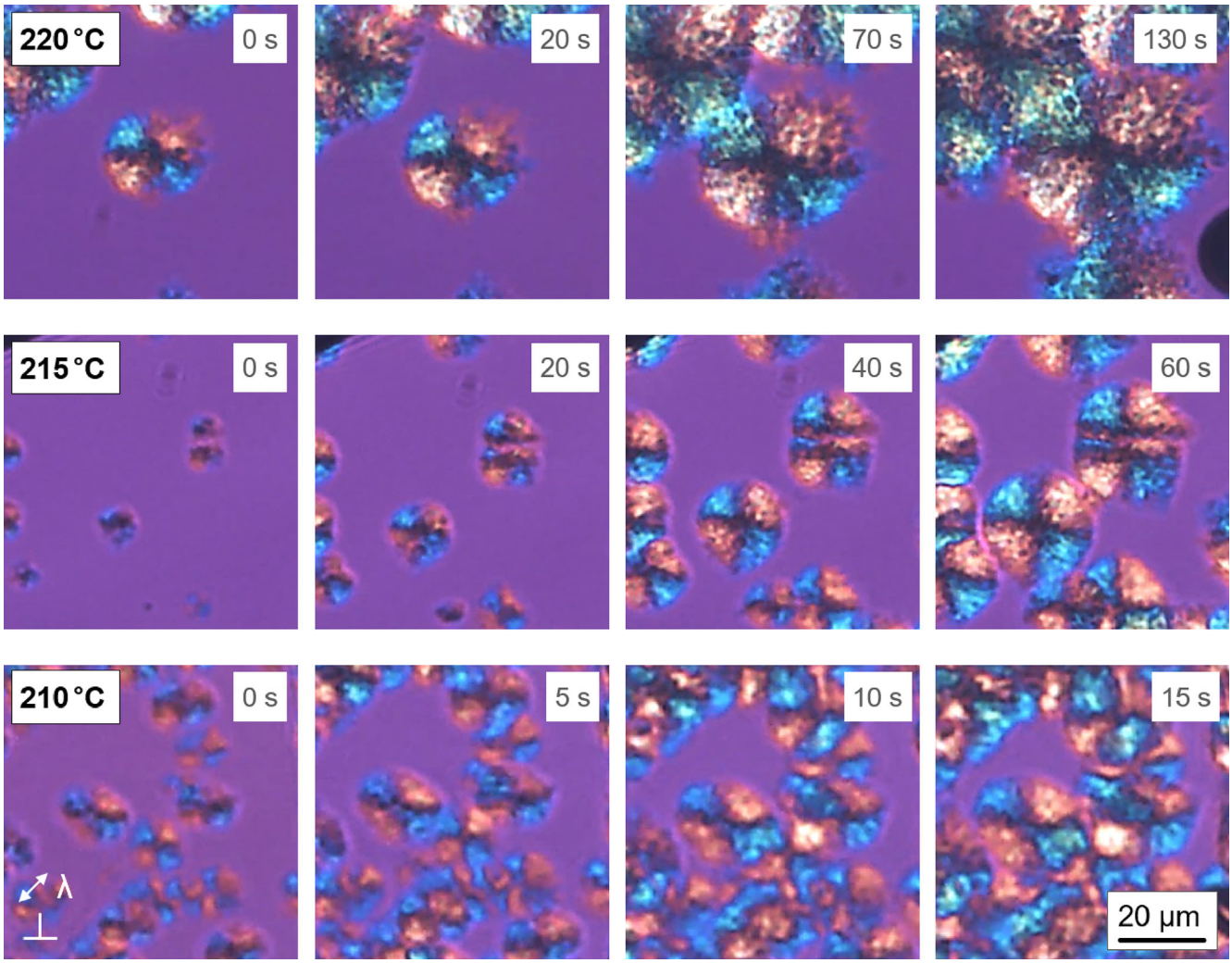

FIGURE 1 Growth of typical α-phase spherulites at temperatures of 210 (bottom row) and 215°C (center row), and of spherulites containing α- and β′-crystals at 220°C (top row), with the images captured after different crystallization time, as indicated. Note that the initial crystallization time (0 s) (shown in each image) is selected arbitrarily, just to indicate the time scale for monitoring the growth process. Before crystallization, samples were heated to 290°C to obtain an equilibrated melt, and cooled at 50 K/min to the crystallization temperature. For each experiment a new sample was employed. The directions of the polarizers and of the λ-plate are indicated in the bottom left image. The scale bar holds for all micrographs.

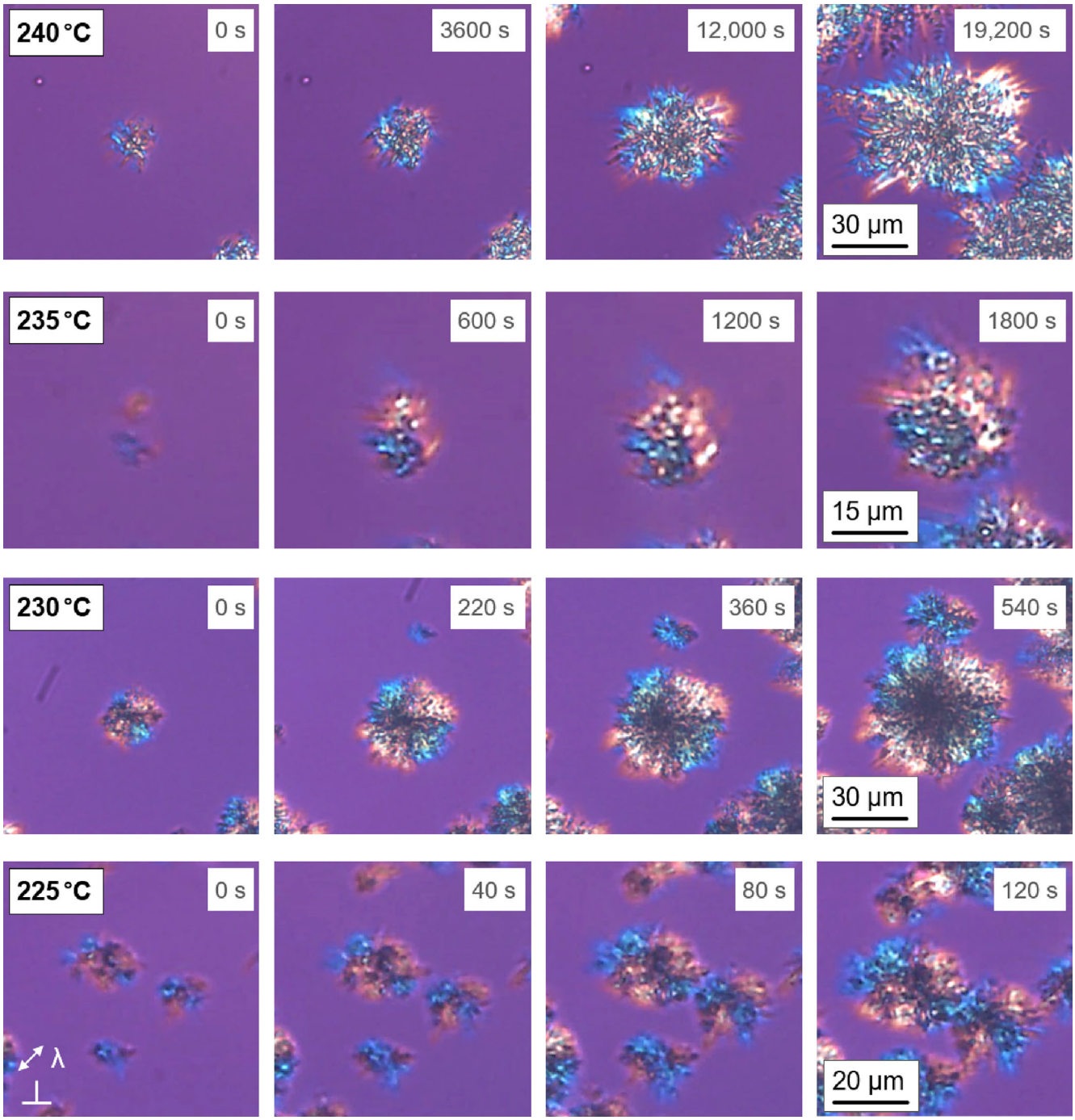

FIGURE 2 Growth of typical β′-phase spherulites at temperatures of 225, 230, 235, and 240°C (from bottom to top rows), with the images captured after different crystallization time, as indicated. Note that the initial crystallization time (0 s) (shown in each image) is selected arbitrarily, just to indicate the time scale for monitoring the growth process. Before crystallization, samples were heated to 290°C to obtain an equilibrated melt, and cooled at 10 K/min to the crystallization temperature. For each experiment a new sample was employed. The directions of the polarizers and of the λ-plate are indicated in the bottom left image. The scale bar holds for all micrographs within a row.

with respect to lower crystallization temperatures (Figure 1) is found. In fact, the spherulites present an uneven and rather jaggy surface caused by the slow dendritic growth of needle-like crystals, being in qualitative contrast to the almost perfect circular/spherical surface of classical spherulites.[45,46] Such morphology is typical of β′-phase crystals.[39,40] Although, there are traces of negative birefringence, patches of non-birefringent zones are present inside the spherulites, perhaps caused by the curly nanoscale morphology of the β′-phase.[40] At such

low supercoolings of the melt, the nucleation density is further reduced with respect to the situation depicted with the top row of Figure 1, and only one or few dendritically grown spherulites are visible in the field-of-view of the micrographs collected at 230°C, or higher temperatures.

Images as exemplarily shown in Figures 1 and 2 served for measurement of the radius of selected spherulites as a function of the crystallization time, with the obtained slope yielding the linear spherulite growth rate, plotted in Figure 3 as a function of the crystallization temperature. Black squares and red circles represent data obtained on spherulites containing β′- and α-crystals, respectively, with the error bar based on analysis of at least three samples. For comparison, the plot also contains a data point (star symbol) obtained on different PBN grade,[44] which, however, fits well the results of this work. The spherulite growth rate, which typically is interpreted as lateral crystal growth rate,[47] decreases with increasing crystallization temperature, from, roughly, 0.3 μm/s at 210°C to less than 0.002 μm/s at 240°C, spanning almost three orders of magnitude in the investigated temperature range from 210 to 240°C. Furthermore, there is observed that the growth rates of the two polymorphs of interest are close to each other at the temperature where β′-crystal growth is replaced by α-crystal growth on decreasing temperature, at around 220–225°C. Unfortunately, the data do not allow prediction of a cross-over of the growth rates of the two polymorphs by extrapolation, even if suggested by the different equilibrium melting temperatures. Rather than, the spherulite growth rates of the two polymorphs are close to fit a single temperature-dependence, allowing to judge cross-nucleation, described below, from a different perspective than different growth rates as a major criterion, frequently posed in the literature. Yellow/orange filled symbols represent data obtained in cross-nucleation experiments, described below.

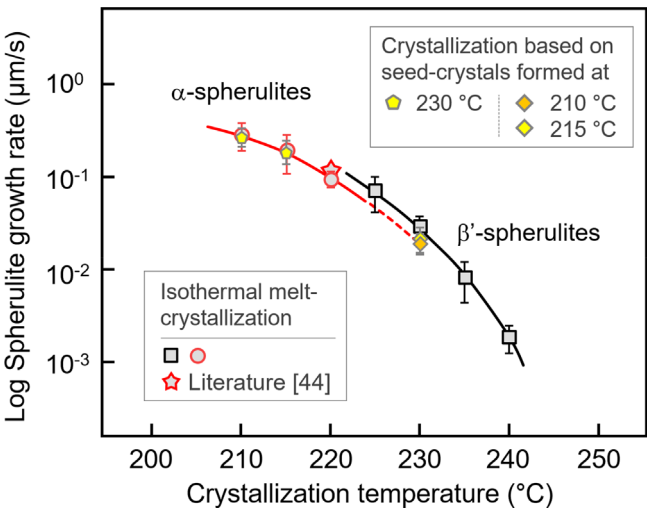

FIGURE 3 Linear growth rate of spherulites containing β′-crystals (black squares), or α-crystals (red circles), as a function of temperature. For each temperature, measurements were performed three times, to assure reproducibility. For comparison, the plot also contains a data point (star symbol) obtained on a different PBN grade.[44] Yellow/orange filled symbols refer to cross-nucleation experiments, showing the crystal-growth rate of spherulites formed at seed-formation temperatures of 210/215 and 230°C, as indicated in the legend.

3.2 | Cross-nucleation/sequential crystallization by hotstage POM

Figure 4 shows the temperature–time profile of performed cross-nucleation experiments, using hotstage microscopy. At first, the thermal history of the sample was removed, by annealing the polymer at 290°C for 3 min, before cooling the equilibrated melt at 50 K/min to pre-selected temperatures of 210 and 215°C, or 230°C, to grow α- or β′-seed crystals, respectively (see blue segment). The annealing time at the seed-formation temperature was adjusted such to assure presence of a sufficiently large fraction of bulk amorphous phase, that is, amorphous structure outside spherulites, before fast transfer of the system to the cross-nucleation temperature (red segments) of 230°C, or 210 and 215°C, to monitor the continuation of the initially incomplete crystallization process.

Figure 5 shows in the left column POM images obtained after incomplete crystallization at seed temperatures of 210 and 215°C, to obtain spherulites containing α-crystals (top two images) and 230°C, to obtain spherulites containing β′-crystals (bottom two images). The images to the right were then collected as a function of

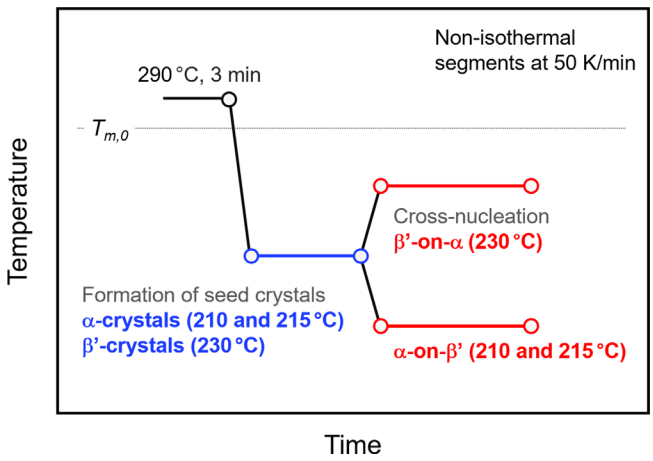

FIGURE 4 Temperature–time profiles of cross-nucleation experiments.

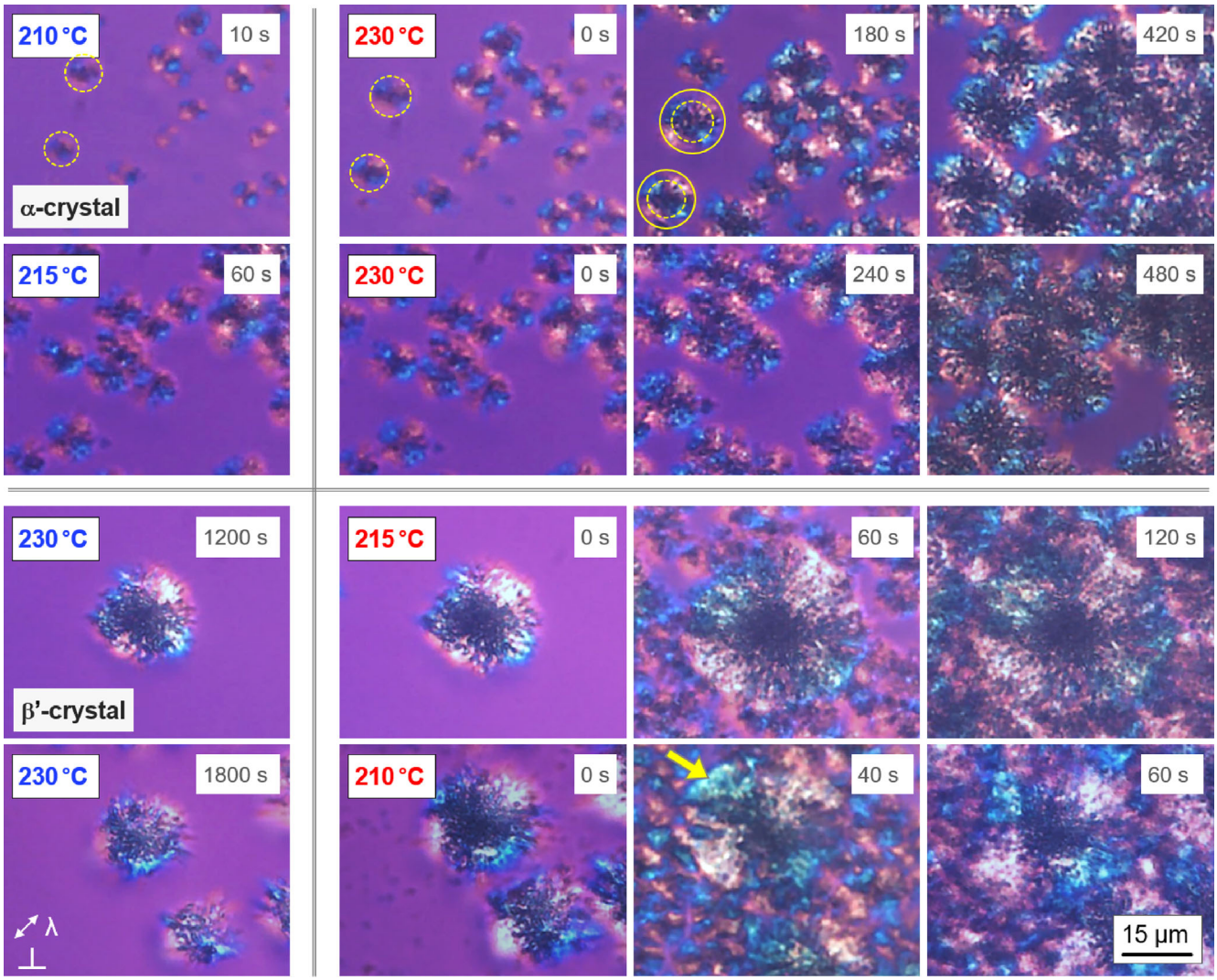

FIGURE 5 POM analysis of cross-nucleation in PBN. Images of the left column were collected at the temperature of seed-crystal formation (see also blue segment in Figure 4), while images to the right illustrate continuation of the initially incomplete crystallization process after transfer of the system to the cross-nucleation temperature (see red segments in Figure 4). The top and bottom two rows of images refer to cross-nucleation experiments using α- and β′-seed crystals, respectively. The directions of the polarizers and of the λ-plate are indicated in the bottom left image. The scale bar holds for all micrographs.

time after the transfer to the respective cross-nucleation temperatures, as indicated in each image.

Regarding the cross-nucleation experiment on α-seed crystals (top two rows), first of all, it is noted that despite the observation of classical negatively birefringent spherulites, which indicates α-crystal formation, the spherulite centers, for unknown reason, appear becoming decorated, as already seen in Figure 1. As will be shown below, X-ray analysis of the crystallization process at 210°C does not reveal any evidence of growth of β′-crystals, which may be related to its negligible fraction. After transfer of spherulites to 230°C, they continue to grow, as illustrated with the dash and solid circles for two selected spherulites, however, cross-nucleation at their perimeter/boundary is not detected. Rather than, the initial decoration, seen already in the center of spherulites grown at 210 and 215°C, continues further, perhaps indicating β′-crystal formation by a solid–solid phase transition, proceeding radially within the spherulites. Similar intraspherulitic transitions have also been reported for the α-phase of poly(vinylidene fluoride) spherulites, undergoing a transition to the more stable γ-phase at high temperature,[48] or for poly(1,3-dioxolan), where phase IIa crystals transform to phase IIb crystals.[20] A further interpretation of this phenomenon may be partial melting of less stable α-crystals formed at 210 or 215°C, followed by reorganization, regardless whether in the transfer stage of the thermal protocol or isothermally during annealing at the cross-nucleation temperature. Such crystal-reorganization process on heating is

common and has been reported for numerous polymers,[2,49–51] including PBN, however, for the latter case without a change of crystal structure.[52] The observed decoration may also be caused by development of β′-crystals in interlamellar amorphous volume, within the existing spherulites.

Qualitatively different sequential-crystallization behavior is observed for the case of transferring β′-seed crystals formed at 230°C to lower temperature of 210 or 215°C, as illustrated with the images of the bottom two rows. The originally grown, at the edge rugged appearing β′-spherulites, continue to grow such to develop the classical spherulite morphology, typical of the α-phase (see yellow arrow). Also here, similar as on heating α-seed crystals, but in contrast to other cases of cross-nucleating polymers,[22–25,27] individual cross-nucleation sites at the surface of the initial β′-spherulites cannot be identified, suggesting an extremely high nucleation density, or simple continuation of growth of the initial β′-crystal lamellae by secondary nucleation, but in a different crystal structure. Apparently, β′-spherulites act similar as classical nucleators, reducing the free-enthalpy barrier for crystal nucleation. Comparing continuation of the crystallization after cooling to 215 and 210°C, it seems that at lower temperature the cross-nucleated α-phase "corona" around the β′-spherulite core appears clearer, with distinct birefringence and observation of a Maltese cross. At higher temperature of 215°C, the newly grown the α-phase again becomes decorated, presumably linked to the presence of a mixed structure composed of α- and β′-crystals in those regions. As shown with the yellow/orange-filled small symbols in Figure 3, the growth rate of spherulites, after their transfer to the cross-nucleation temperature, is similar to spherulites isothermally grown in the bulk melt without a prior nucleation- and growth-step at different temperature (black squares/red circles).

3.3 | Cross-nucleation/sequential crystallization by temperature-resolved WAXS

Analysis of possible cross-nucleation on sequential crystallization of PBN at different temperatures by temperature-resolved WAXS served for unequivocal detection of formation of specific crystal polymorphs since the morphological data obtained by hotstage microscopy are considered supportive only. Before analyzing sequential crystallization, isothermal crystallization experiments at 210 and 230°C were performed, to prove formation of α- and β′-crystals, respectively. As such, Figure 6 shows WAXS curves, intensity as a function of the scattering angle 2θ, recorded during isothermal crystallization of

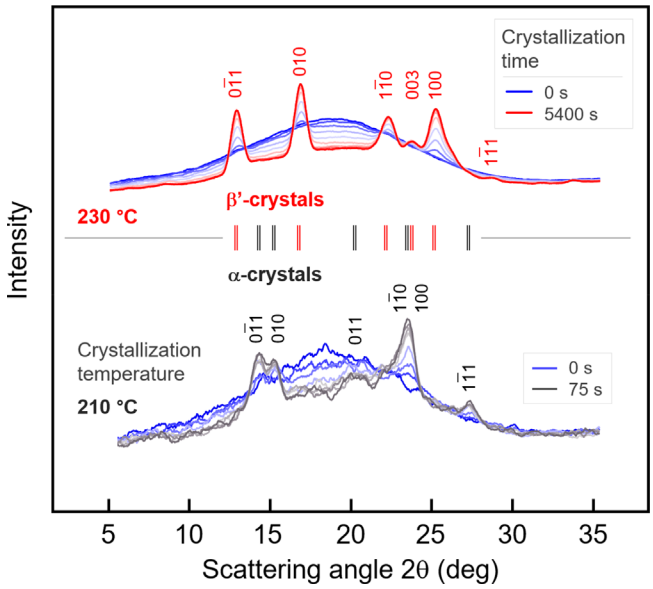

FIGURE 6 WAXS curves recorded during isothermal crystallization of PBN at 230°C (top set of curves) or 210°C (bottom set of curves). The melt was cooled from 280°C to the target temperature at a rate of 30 K/min. Related to different crystallization rate, the time increment between two subsequent measurements is about 600 and 13 s for crystallization at 230 and 210°C, respectively. Peaks were indexed according to the literature.[36,53]

PBN at 210°C (bottom set of curves) or 230°C (top set of curves). In both cases, the equilibrated melt was cooled from 280°C to the target temperature at a rate of 30 K/min, and then X-ray frames/curves were collected every 600 s on crystallization at 230°C, and 13 s on crystallization at 210°C, related to the largely different crystallization rate at these temperatures. The much shorter exposure time during crystallization at 210°C then also caused the larger noise of data. The dark blue curves in both curve sets represent the first measurement after the crystallization temperature was reached, confirming absence of scattering peaks and presence of an amorphous-phase halo only. With increasing crystallization time, scattering peaks evolve and increase in intensity, caused by the increasing crystal fraction. Roughly, crystallization at 210 and 230°C appeared finished after about 1–2 min and 1–2 h, respectively. However, most important in the context of the present study, is the confirmation that crystallization of the non-seeded melt at 210 and 230°C yields exclusively α- and β′-crystals, respectively, as deduced from the analysis of the position of the scattering peaks, indexed according to the literature.[36,53]

Figure 7 shows WAXS curves recorded during annealing PBN at 230°C up to about 60 min, representing the β′-on-α cross-nucleation step in Figure 4 (upper red segment). Before recording the WAXS data, PBN was

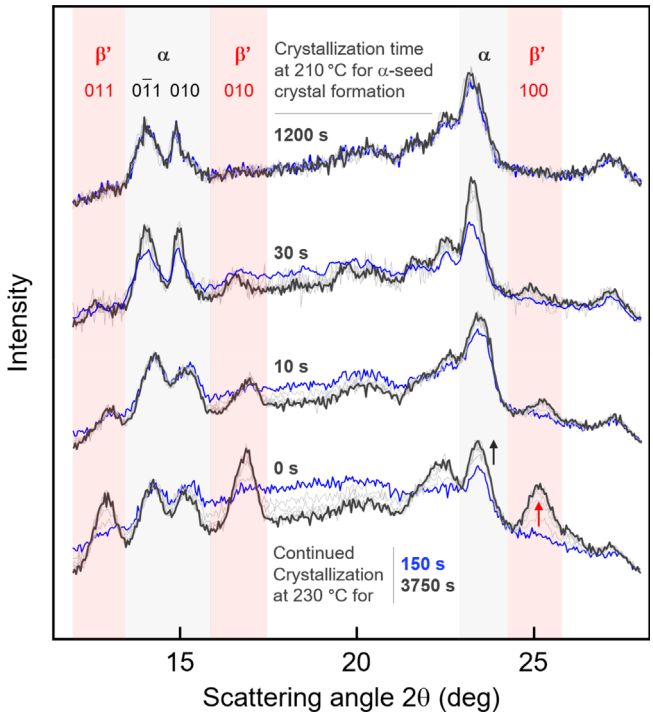

FIGURE 7 WAXS curves recorded during annealing PBN at 230°C up to about 60 min, after prior crystallization at 210°C for 0, 10, 30, and 1200 s (from bottom to top curve sets). The melt was cooled from 270 to 210°C at 30 K/min, subjected to crystallization/α-seed-crystal formation for different time, and then heated to 230°C at 30 K/min, to continue the crystallization process. The measurement–time for each curve was 300 s and the time increment between two subsequent measurements at 230°C is 600 s. For illustration of growth of different polymorphs at 230°C, selected peaks are indexed. Curve sets are shifted vertically for the sake of clarity, without changing the relative intensity scale.

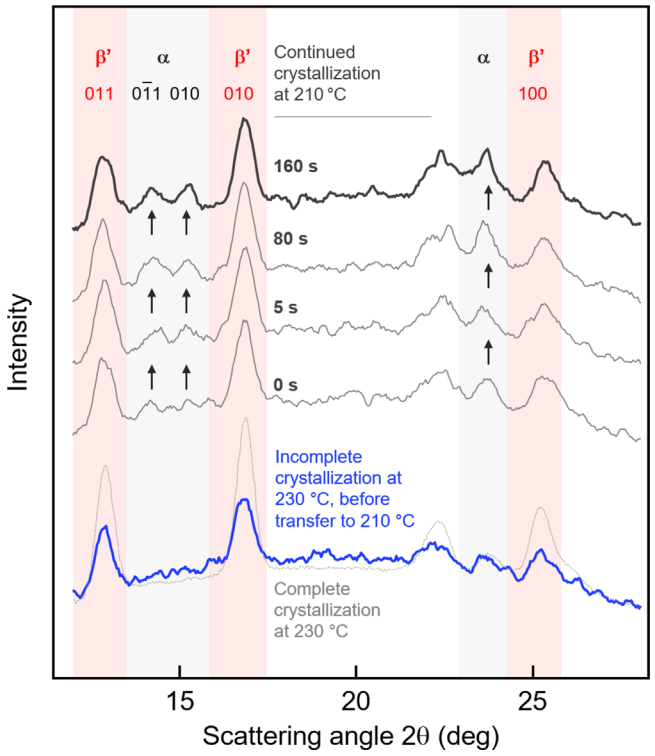

FIGURE 8 WAXS curves recorded during annealing PBN at 210°C up to 160 s (upper four curves), after prior incomplete crystallization at 230°C (blue curve). The melt was cooled from 270 to 230°C at 30 K/min, subjected to crystallization/β′-seed-crystal formation for 60 min, and then cooled to 230°C at 30 K/min, to continue the crystallization process. The incompleteness of crystallization at 230°C, to leave space for seed-assisted crystallization at 210°C, is demonstrated with the gray dash line, showing the intensity of β′-peaks after complete crystallization for 120 min. For illustration of growth of different polymorphs at 230°C, selected peaks are indexed. Curves are shifted vertically for the sake of clarity, without changing the relative intensity scale.

crystallized at 210°C for 0, 10, 30, and 1200 s (from bottom to top curve sets), for generation of α-seed-crystals (see the blue segment in Figure 4). PBN was crystallized at 210°C for different time for obtaining samples of different crystallinity, that is, fraction of bulk amorphous phase before continuation of crystallization at 230°C. As such, crystallization at 210°C for 0 s yielded an almost fully amorphous sample (see blue curve in the bottom curve set), with the weak α-crystal peaks probably caused by crystallization during heating the system to 230°C. Most striking, however, is further formation of α-crystals, besides the expected β′-crystal growth, as indicated with the black and red arrows on two selected scatterings peaks associated to α- and β′-crystals, respectively. With increasing crystallization time at 210°C to 10 and 30 s, the initial α-crystal fraction at 230°C increases, however, also in these cases continued formation of both α- and β′-crystals is observed. Finally, as shown with the top curve set, annealing of PBN at 210°C for 1200 s allows completion of the crystallization process and further changes of the structure after heating to 230°C are not detected.

The data of Figure 7 confirm the hotstage-POM experiment of Figure 5 (upper row images). There, α-seed crystals were grown for a period of 10 s, leading to a non-space-filled spherulitic structure, that is, to formation of few isolated spherulites embedded in the liquid melt. After transfer of the system to 230°C, the spherulites containing α-crystals continued to grow in the α-phase, as concluded by their unchanged appearance (see yellow circles). Simultaneously, starting from the center of the spherulites, they become decorated which either indicates partial transformation of α- into β′-crystals, or their new formation in intraspherulitic spaces from the melt.

Finally, Figure 8 provides information about sequential crystallization starting with incomplete formation of

β′-crystals at 230°C for 60 min, transfer of the system to 210°C and continuation of the crystallization process at this temperature, as gained by WAXS. The blue curve was collected at 230°C, just before cooling the sample to 210°C, revealing presence of β′-crystals. With the gray dash curve, measured using the same sample for a period of 120 min, is confirmed that crystallization for 60 min is incomplete, since the intensity of the peaks at the end of crystallization process is further increased. As such, the sample, before the transfer to 210°C, leaves sufficient space for continuation of crystallization at 210°C. The top four curves in Figure 8, from bottom to top, show the evolution of the structure at 210°C. It appears that the intensity of the β′-peaks increased slightly in intensity during the transfer of the system from 230 to 210°C (see curve labeled "0 s"), however, then, during the course of the annealing process at 210°C, a further increase of the fraction of β′-crystals is not detected. Instead, α-crystal formation is indicated by the appearance of their characteristics scattering peaks, as indicated with the vertical black arrows. After few minutes, the crystallization process seems finished, because of the fast growth of the α-phase.

The data of Figure 8 are in agreement with the hotstage-POM cross-nucleation experiment of Figure 5 (bottom two rows). The bottom left image revealed presence of a large bulk (outside of spherulites) amorphous fraction of crystallization of the PBN at 230°C for 30 min, being a necessary pre-requisite to allow continuation of crystallization at 210°C. After the transfer of the system to 210°C, both continuation of growth of existing spherulites (see yellow arrow) without detection of specific (primary) nucleation points at their boundaries, and formation of new spherulites in the bulk amorphous phase by α-crystal formation was detected. This confirms the hotstage POM experiment of Figure 5 (bottom-row image), which suggested that only α-crystals grow at the edge of β′-seed crystals.

The in-situ WAXS cross-nucleation experiments provide further insight about the growth of the various polymorphs of PBN and in presence of specific seed-crystals. In particular, β′-on-α cross-nucleation experiments demonstrate that, in addition to the expected β′-phase formation in the crystallization temperature range where its formation is kinetically and thermodynamically favored, α-crystals continue to grow on the α-seed, even at temperatures where the non-seeded melt develops the β′-phase only. On the other hand, α-on-β′ sequential-crystallization experiments show that the opposite situation does not occur, as cross-nucleation of the α-phase on the β′-structure is exclusively observed at lower temperatures. Apparently, in this latter case, there is a kinetic advantage of growth of the metastable α-phase, compared to growth of β′-crystals, due to the higher applied supercooling.

4 | CONCLUSIONS

In this work, the possibility of cross-nucleation between the different crystal polymorphs of poly(butylene 2,6-naphthalate) on changing the crystallization conditions is explored, using an in-situ seeding strategy, and adopting hotstage polarized-light optical microscopy and temperature-resolved wide angle X-ray scattering. PBN forms β′- and α-crystals on crystallization of the non-seeded melt at temperatures lower and higher than about 220–225°C, respectively, with their growth rates being very similar at temperatures where both polymorphs develop. Presence of dendritically grown β′-seed crystals in the bulk melt, at temperatures where typically α-crystals grow, allows cross-nucleation at the edge of the β′-spherulites, that is, there is observed a switchover of the crystal structure. In contrast, α-phase seed-spherulites, formed at relatively low temperature and transferred together with non-crystallized bulk amorphous structure to high temperature, continues to grow without a change of the crystal structure. In parallel, β′-structure begins to form at the center of the α-phase spherulites, radially continuing and competing with the further growth of the α-seed until impingement.

The data suggest that the growth face of α-crystals, regardless temperature, relative thermodynamic stability, and minor differences of growth rates of the various crystal polymorphs, favors secondary nucleation in the same crystal structure. For the β′-phase, such behavior is not observed as seed-crystals cannot enforce growth in the same structure at temperatures where bulk-melt crystallization yields a different polymorph. As we consider the present knowledge about the relative thermodynamic stability of the various phases, including their equilibrium melting temperatures, and about the specific structure of crystal-growth fronts—controlling secondary nucleation barriers and epitaxy—still not sufficiently investigated, further in-depth interpretation of the observations gained in this work is not possible. This notwithstanding, the performed experiments underline the importance of the structure of (heterogeneous) secondary nuclei on growth of specific crystal polymorphs, with this knowledge applicable for tailoring of semicrystalline morphologies.

ACKNOWLEDGMENTS

RA acknowledges funding by the Deutsche Forschungsgemeinschaft (DFG) (grant AN 212/29). MD thanks for financial support by the Martin Luther University

Halle-Wittenberg, and fruitful discussions of research results with Prof. J. Ulrich (Martin Luther University Halle-Wittenberg).

ORCID

Dario Cavallo https://orcid.org/0000-0002-3274-7067

REFERENCES

[1] B. H. Clampitt, R. Hughes, *J. Polym. Sci. Polym. Symp.* **1964**, *6*, 43.
[2] R. Androsch, C. Schick, M. L. Di Lorenzo, *Macromol. Chem. Phys.* **2014**, *215*, 1134.
[3] F. Azzurri, A. Flores, G. C. Alfonso, I. Sics, B. S. Hsiao, F. B. Calleja, *Polymer* **2003**, *44*, 1641.
[4] K. Jariyavidyanont, Q. Yu, A. Petzold, T. Thurn-Albrecht, R. Glüge, H. Altenbach, R. Androsch, *J. Mech. Behav. Biomed. Mater.* **2023**, *137*, 105546.
[5] L. Shen, I. Y. Phang, T. Liu, *Polym. Test.* **2006**, *25*, 249.
[6] E. Fukada, T. Furukawa, *Ultrasonics* **1981**, *19*, 31.
[7] Y. S. Choi, S. K. Kim, F. Williams, Y. Calahorra, J. A. Elliott, S. Kar-Narayan, *Chem. Commun.* **2018**, *54*, 6863.
[8] B. Wunderlich, *Macromolecular Physics. Crystal Nucleation, Growth, Annealing*, Vol. 2, Academic Press, New York **1976**.
[9] C. Schick, R. Androsch, J. W. P. Schmelzer, *J. Phys. Cond. Matter* **2017**, *29*, 453002.
[10] G. Tammann, *Z. Phys. Chem.* **1898**, *25*, 441.
[11] E. Zhuravlev, J. W. P. Schmelzer, A. S. Abyzov, V. M. Fokin, R. Androsch, C. Schick, *Cryst. Growth Des.* **2015**, *15*, 786.
[12] R. Androsch, Homogenous crystal nuclei in poly (L-lactic acid), formed at 60°C, grow to both α′- and α-crystals, depending on the growth temperature, unpublished data, **2023**.
[13] W. Stocker, M. Schumacher, S. Graff, A. Thierry, J. C. Wittmann, B. Lotz, *Macromolecules* **1998**, *31*, 807.
[14] A. M. Rhoades, N. Wonderling, A. Gohn, J. Williams, D. Mileva, M. Gahleitner, R. Androsch, *Polymer* **2016**, *90*, 67.
[15] D. J. Blundell, A. Keller, *J. Macromol. Sci., Phys.* **1968**, *2*, 301.
[16] G. Reiter, *Chem. Soc. Rev.* **2014**, *43*, 2055.
[17] L. Sangroniz, D. Cavallo, A. J. Müller, *Macromolecules* **2020**, *53*, 4581.
[18] L. Yu, *J. Am. Chem. Soc.* **2003**, *125*, 6380.
[19] S. Chen, H. Xi, L. Yu, *J. Am. Chem. Soc.* **2005**, *127*, 17439.
[20] C. Fraschini, L. Jiménez, B. Kalala, R. E. Prud'homme, *Polymer* **2012**, *53*, 188.
[21] Y. Nozue, S. Seno, T. Nagamatsu, S. Hosoda, Y. Shinohara, Y. Amemiya, E. B. Berda, G. Rojas, K. B. Wagener, *ACS Macro Lett.* **2012**, *1*, 772.
[22] D. Cavallo, L. Gardella, G. Portale, A. J. Müller, G. C. Alfonso, *Polymer* **2013**, *54*, 4637.
[23] D. Cavallo, L. Gardella, G. Portale, A. J. Müller, G. C. Alfonso, *Macromolecules* **2014**, *47*, 870.
[24] D. Cavallo, F. Galli, L. Yu, G. C. Alfonso, *Cryst. Growth Des.* **2017**, *17*, 2639.
[25] D. Cavallo, G. C. Alfonso, *Adv. Polym. Sci.* **2015**, *277*, 1.
[26] A. J. Lovinger, J. O. Chua, C. C. Gryte, *J. Polym. Sci. Part A: Polym. Phys.* **1977**, *15*, 641.
[27] W. Wang, B. Wang, S. F. S. P. Looijmans, E. Carmeli, M. Rosenthal, G. Liu, D. Cavallo, *Macromolecules* **2021**, *54*, 9663.
[28] S. Looijmans, A. Menyhard, G. W. Peters, G. C. Alfonso, D. Cavallo, *Cryst. Growth Des.* **2017**, *17*, 4936.
[29] Q. Ding, M. Soccio, N. Lotti, D. Cavallo, R. Androsch, *Chin. J. Polym. Sci.* **2020**, *38*, 311.
[30] T. Konishi, K. Nishida, G. Matsuba, T. Kanaya, *Macromolecules* **2008**, *41*, 3157.
[31] W. Ostwald, *Z. Phys. Chem.* **1897**, *22*, 289.
[32] T. Threlfall, *Org. Proc. Res. Dev.* **2003**, *7*, 1017.
[33] D. Cavallo, D. Mileva, G. Portale, L. Zhang, L. Balzano, G. C. Alfonso, R. Androsch, *ACS Macro Lett.* **2012**, *1*, 1051.
[34] R. Androsch, M. Soccio, N. Lotti, D. Cavallo, C. Schick, *Thermochim. Acta* **2018**, *670*, 71.
[35] H. Koyano, Y. Yamamoto, Y. Saito, T. Yamanobe, T. Komoto, *Polymer* **1998**, *39*, 4385.
[36] A. E. Tonelli, *Polymer* **2002**, *43*, 6069.
[37] M. Soccio, N. Lotti, L. Finelli, A. Munari, *Polym. J.* **2012**, *44*, 174.
[38] M. Yasuniwa, S. Tsubakihara, T. Fujioka, Y. Dan, *Polymer* **2005**, *46*, 8306.
[39] M. Y. Ju, F. C. Chang, *Polymer* **2001**, *42*, 5037.
[40] M. Du, A. Janke, K. Jariyavidyanont, R. Androsch, *Mater. Lett.* **2023**, *333*, 133570.
[41] Q. Ding, D. Jehnichen, M. Göbel, M. Soccio, N. Lotti, D. Cavallo, R. Androsch, *Eur. Polym. J.* **2018**, *101*, 90.
[42] Q. Ding, A. Janke, C. Schick, R. Androsch, *Polymer* **2020**, *194*, 122404.
[43] Q. Ding, M. Du, T. Liao, Y. Men, R. Androsch, *Polymer* **2022**, *257*, 125275.
[44] D. G. Papageorgiou, D. N. Bikiaris, G. Z. Papageorgiou, *CrystEngComm* **2018**, *20*, 3590.
[45] J. H. Magill, *J. Mater. Sci.* **2001**, *36*, 3143.
[46] B. Crist, J. M. Schultz, *Progr. Polym. Sci.* **2016**, *56*, 1.
[47] J. D. Hoffman, J. I. Lauritzen Jr., *J. Res. Nat. Bur. Stand. Sect. A: Phys. Chem.* **1961**, *65*, 297.
[48] A. J. Lovinger, *Polymer* **1980**, *21*, 1317.
[49] A. A. Minakov, D. A. Mordvintsev, C. Schick, *Polymer* **2004**, *45*, 3755.
[50] A. A. Minakov, D. A. Mordvintsev, R. Tol, C. Schick, *Thermochim. Acta* **2006**, *442*, 25.
[51] K. Jariyavidyanont, R. Androsch, C. Schick, *Polymer* **2017**, *124*, 274.
[52] M. Yasuniwa, S. Tsubakihara, T. Fujioka, *Thermochim. Acta* **2003**, *396*, 75.
[53] M. Y. Ju, J. M. Huang, F. C. Chang, *Polymer* **2002**, *43*, 2065.

How to cite this article: M. Du, R. Androsch, D. Cavallo, *J. Polym. Sci.* **2024**, *62*(9), 1789. https://doi.org/10.1002/pol.20230810